RESEARCH ARTICLE SUMMARY

PALEONTOLOGY

Sexual selection promotes giraffoid head-neck evolution and ecological adaptation

Shi-Qi Wang*, Jie Ye, Jin Meng*, Chunxiao Li, Loïc Costeur, Bastien Mennecart, Chi Zhang, Ji Zhang, Manuela Aiglstorfer, Yang Wang, Yan Wu, Wen-Yu Wu, Tao Deng*

INTRODUCTION: Extreme evolution of animal organs, such as elongation of the giraffe's neck, has been the focus of intensive research for many decades. Here, we describe a fossil giraffoid, *Discokeryx xiezhi*, from the early Miocene (~16.9 million years ago) of northern China. This previously unknown species has a thick-boned cranium with a large disklike headgear, a series of cervical vertebrae with extremely thickened centra, and the most complicated head-neck joints in mammals known to date. The peculiar head-neck morphology was most probably adapted for a fierce intermale head-butting behavior, comparable to neck-blowing in male giraffes but indicative of an extreme adaptation in a different direction within giraffoids. This newly identified giraffoid increases our understanding the actual triggers for the giraffe's head-neck evolution.

RATIONALE: The comparative anatomical studies of osteological structures, including the bony labyrinth morphology, the headgear genesis and histology, and dentitions, provide the basis for the giraffoid affinity of *D. xiezhi*, which was further supported by phylogenetic analyses and reconstructions of the fauna. Finite element analyses explain the mechanical predominance for the peculiar head-neck morphology in various head-butting modeling. Tooth enamel isotope analyses indicate the distinctiveness of the ecological niche occupied by *D. xiezhi*. Diversity of headgear within different pecoran groups reveals the different evolutionary selection pressure on these groups.

RESULTS: Finite element analysis reveals that the enlarged atlanto-occipitalis and intercervical articulations are essential for high-speed head-to-head butting. *D. xiezhi* appears to exhibit the most optimized head-butting adaptation in vertebrate evolution when compared with the models of extant head-butters. Tooth enamel isotope data show that *D. xiezhi* had the second highest average $\delta^{13}C$ value among all herbivores and a large range of $\delta^{18}O$ values, with some individuals occupying an isotopic niche differing substantially from others in the fossil community. This indicates that *D. xiezhi* was an open-land grazer with multiple sources of water intake, and their habitats likely included areas that were difficult for other contemporary herbivores to make use of.

CONCLUSION: The morphology and inferred ecology of *D. xiezhi* provide another example for understanding the neck evolution in giraffoids. Fossil giraffoids exhibit a higher degree of diversity in headgear morphology than any other pecoran group; such a diversity, associated with the complex head-neck morphology, likely indicates the intensive sexual combats between males in the evolution of giraffoids. For interspecific relationship, one possible strategy of early giraffoids is that they might have avoided competition with coeval bovids and cervids by taking advantage of other niches in the ecosystem. *Giraffa*,with its long neck, did not appear until the early Pliocene in savannah areas, when C_4 ecosystems started being vastly established. "Necking" combat was likely the primary driving force for giraffes that have evolved a long neck, and high-level browsing was likely a compatible benefit of this evolution. The ecological positioning on the marginal niches promoted the intensive sexual competition, and the fierce sexual combats fostered extreme morphologies to occupy the special niches in giraffoids. ■

The list of author affiliations is available in the full article online.
*Corresponding author. Email: wangshiqi@ivpp.ac.cn (S.-Q.W.); jmeng@amnh.org (J.M.); dengtao@ivpp.ac.cn (T.D.)
Cite this article as S.-Q. Wang *et al.*, *Science* **376**, eabl8316 (2022). DOI: 10.1126/science.abl8316

READ THE FULL ARTICLE AT
https://doi.org/10.1126/science.abl8316

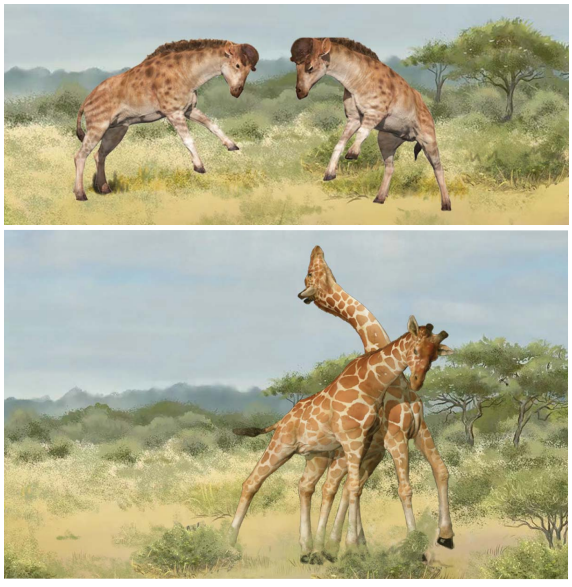

ILLUSTRATION: Y. WANG AND X. GUO

Male combat in the representative giraffoids. *D. xiezhi* (head-to-head butting, top left) and the extant *Giraffa camelopardalis* (neck blowing, bottom left) show different combat styles and head-neck morphology. The right panel exhibits the accumulative number of headgears in various pecoran groups during their evolution. Note that giraffomorphs had evolved more types of headgear than other pecoran groups, which may be partly attributable to their various combat styles.

RESEARCH ARTICLE

PALEONTOLOGY

Sexual selection promotes giraffoid head-neck evolution and ecological adaptation

Shi-Qi Wang[1,2]*, Jie Ye[1,2], Jin Meng[3]*, Chunxiao Li[1,2,4], Loïc Costeur[5], Bastien Mennecart[5,6], Chi Zhang[1,2], Ji Zhang[7,8], Manuela Aiglstorfer[9], Yang Wang[10,11], Yan Wu[1,2], Wen-Yu Wu[1,2], Tao Deng[1,2,4]*

The long neck of the giraffe has been held as a classic example of adaptive evolution since Darwin's time. Here we report on an unusual fossil giraffoid, *Discokeryx xiezhi*, from the early Miocene, which has an unusual disk-shaped headgear and the most complicated head-neck joints in known mammals. The distinctive morphology and our finite element analyses indicate an adaptation for fierce head-butting behavior. Tooth enamel isotope data suggest that *D. xiezhi* occupied a niche different from that of other herbivores, comparable to the characteristic high-level browsing niche of modern giraffes. The study shows that giraffoids exhibit a higher headgear diversity than other ruminants and that living in specific ecological niches may have fostered various intraspecific combat behaviors that resulted in extreme head-neck morphologies in different giraffoid lineages.

The extreme elongation of the giraffe's neck has been considered a classical example of adaptive evolution and natural selection since the time of Lamarck and Darwin (*1*, *2*) and has inspired various hypotheses to explain this peculiar feature (*3*). Competition with other browsers for food resources and the "necks-for-sex" hypothesis, in which elongation is related to intermale competition, have been proposed as explanations (*3*, *4*). Testing these mechanisms is difficult, but the fossil record can play a crucial role (*4*). An unusual giraffoid ruminant, *Discokeryx xiezhi* gen. et sp. nov., from the latest early Miocene [~16.9 million years ago (Ma)] was recently recovered in the northern Junggar Basin, China (figs. S1 to S3). This animal exhibits a peculiar head-neck morphology that was most likely related to an extreme sexually related head-butting behavior. Finite element analyses reveal that it might have possessed the most optimized head-butting adaptation in vertebrate evolution. Tooth enamel isotope data for some *D. xiezhi* individuals differ from that of other taxa of the fossil herbivore community. This also suggests that *D. xiezhi* occupied a specific niche in the ecosystem, comparable to extant giraffes that use their elongated necks for combat and browsing at the highest levels of the savannah woodland canopy. These results suggest that biotic factors such as different strategies in sexual combat have acted on the development of giraffoid head-neck morphologies and that distinct ecological positioning played a role in giraffoid morphological evolution and adaptation.

[1]Key Laboratory of Vertebrate Evolution and Human Origins of Chinese Academy of Sciences, Institute of Vertebrate Paleontology and Paleoanthropology, Chinese Academy of Sciences (CAS), Beijing 100044, China. [2]CAS Center for Excellence in Life and Paleoenvironment, Beijing 100101, China. [3]American Museum of Natural History, New York, NY 10024, USA. [4]College of Earth and Planetary Sciences, University of Chinese Academy of Sciences, Beijing 100049, China. [5]Naturhistorisches Museum Basel, 4001 Basel, Switzerland. [6]Naturhistorisches Museum Wien, Vienna 1010, Austria. [7]School of Civil and Hydraulic Engineering, Huazhong University of Science and Technology, Wuhan 430047, China. [8]Department of Civil and Environmental Engineering, University of California, Berkeley, CA 94720, USA. [9]Naturhistorisches Museum Mainz/Landessammlung für Naturkunde Rheinland-Pfalz, 55116 Mainz, Germany. [10]Department of Earth, Ocean, and Atmospheric Science, Florida State University, Tallahassee, FL 32306, USA. [11]National High Magnetic Field Laboratory, Tallahassee, FL 32310, USA.
*Corresponding author. Email: wangshiqi@ivpp.ac.cn (S.-Q.W.); jmeng@amnh.org (J.M.);dengtao@ivpp.ac.cn (T.D.)

Systematics. Superfamily Giraffoidea Hamilton, 1978. Family Prolibytheriidae Sánchez *et al.*, 2019. Genus *Discokeryx* gen. nov. (monotypic genus). **Etymology:** *Disco-*, round plate, *keryx*, horn, indicating the disklike headgear; masculine. **Diagnosis:** Large prolibytheriid with a medially positioned flat disklike headgear supported by the parietal bone. Basicranium extraordinarily enlarged, and ventral arch of the atlas correspondingly thickened, forming a complex surface for head-neck articulation. **Type and the only species:** *Discokeryx xiezhi* sp. nov. [Figs. 1 and 2, A and B; figs. S5 to S10; tables S4 to S8; data S1; and 3D models S1 to S21 (*5*)]. **Etymology:** In Chinese legends, Xiezhi is a one-ossiconed giraffe. **Type specimens:** Holotype: IVPP V26602, braincase and the following four vertebrae, which were articulated in situ; hypodigm: see data S1 and supplementary materials, section 3.1. **Diagnosis:** As for the genus.

Results

The most conspicuous feature of *D. xiezhi* is a single flat, disklike headgear on top of the parietal bone (Fig. 1 and figs. S5 and S6). The headgear tissue is centrifugally accumulated, which forms radial vascular grooves and scattered vascular pores on the dorsal surface, and is seen most clearly in a juvenile individual specimen (Fig. 1H and fig. S6E). The finely roughened surface indicates that a keratinous integument covered the headgear during the animal's lifetime. The keratinous tissue grew within the dermis on the headgear's dorsal surface. Thin layers of new keratinous tissue developed evenly and increasingly coated the headgear's surface. The older layers were pushed outward to form a helmet-shaped structure (Fig. 2A) as the headgear increased in diameter. The bony walls of the neurocranium are very thick (Fig. 1F), probably in response to the head-butting behavior.

D. xiezhi has very unusual atlanto-occipital and intercervical articulations that are extremely enlarged (Fig. 1, C to E, and figs. S5, S6, and S10). The condyles are ventrally fused, and the basicranium is extremely expanded to form a pentagonal "basilar platform." The surfaces of the basilar platform, the condyloid fossae, and the condyles themselves constitute a complicated articulation system. The ventral arch of the atlas is exceedingly hypertrophic, forming a "ventral chunk" with corresponding facets that precisely match with the basilar platform (Fig. 1, C and D, and fig. S10A). Similar to the atlas, the centra of cervical vertebrae II to V are ventrally enlarged, and the transverse processes of cervical vertebrae III and IV are strongly anteriorly expanded, participating in and strengthening the intercervical articulations (Fig. 1E and fig. S10). This cervical configuration is advantageous in impact energy absorption for fierce head-butting.

We performed finite element analyses to simulate the head-neck morphology relative to a presumed head-butting behavior in *D. xiezhi* (Fig. 3, A to D; figs. S4 and S14; Movies 1 to 3; and tables S1 to S3). In the thick cervical model, the original digital geometry incorporating the braincase and the following four cervical vertebrae of *D. xiezhi* were used. In contrast, in the attenuated cervical models, the accessory head-neck articulations were removed from the digital geometry. In the attenuated cervical models, the atlanto-occipital articulation would undergo an unacceptable inflection—an excessive rotation of up to 54.7° (Fig. 3, A to C). When a 5° rotation limit for the atlanto-occipital rotation was enforced, the time history curves of strain energy (THCSE) peak values of each bone in the attenuated cervical model were notably higher than those of the thick cervical model, particularly for the atlas, for which the values were at least five times higher than those of the thick cervical model (Fig. 3D). Such increases would greatly raise the risk of bone damage. The finite element analyses suggest that the highly specialized head-neck morphology in *D. xiezhi* could indeed be related to intense head-butting behavior. An enlarged atlanto-occipital articulation (but not

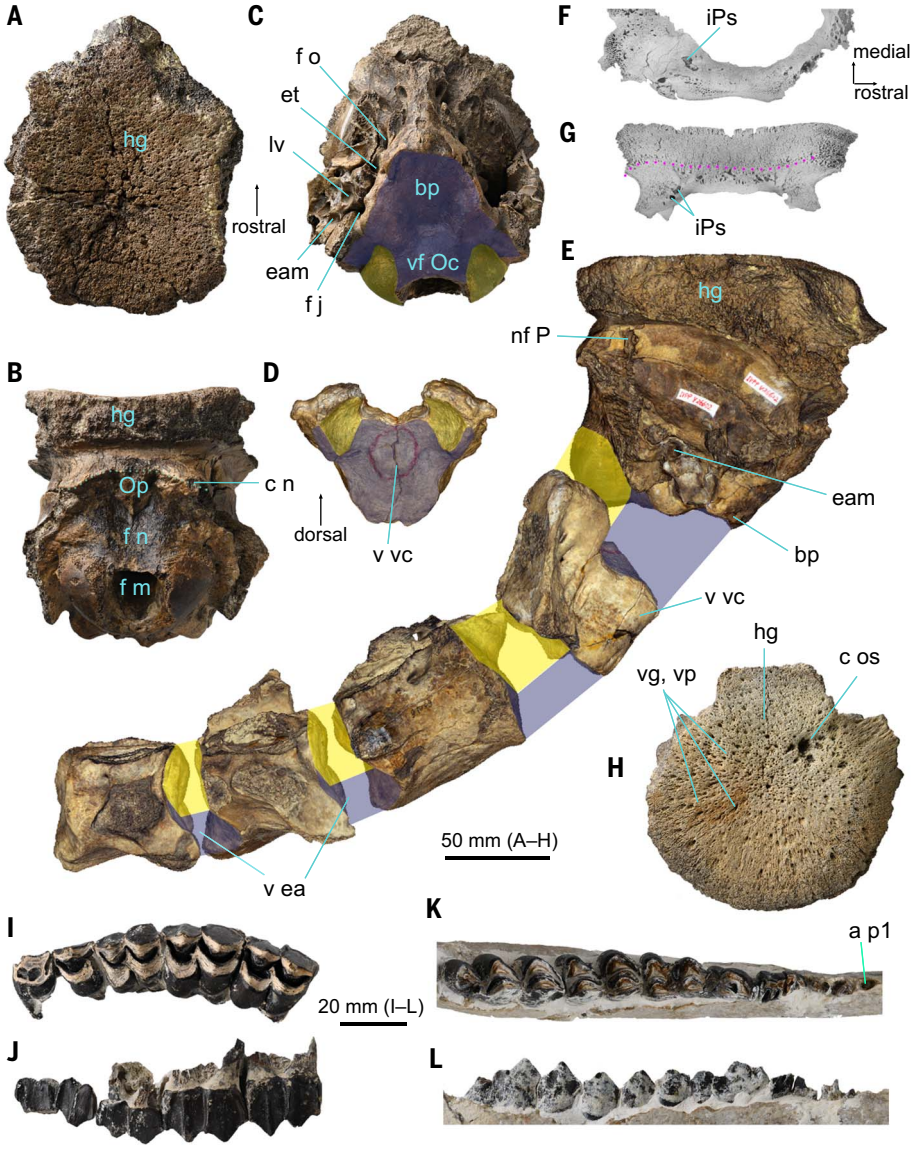

Fig. 1. *D. xiezhi* gen. et sp. nov. (**A** to **F**) IVPP V26602, the type specimen, showing the dorsal view of the braincase (A), emphasizing the disklike headgear; the caudal view of the braincase (B), emphasizing the concaveness of the occipital bone, as well as the strong and medially depressed nuchal crest; the ventral view of the braincase (C), emphasizing the extraordinarily expanded basilar platform; the cranial view of the atlas (D), emphasizing the ventral trunk articulated to the basilar platform in (C); the lateral view of the braincase articulated with the following four cervical vertebrae (CVs) (E), emphasizing the thick CVs and extra articulations (the yellow shadows delineate the regular articulatory areas in common mammals, and the purple shadows indicate the extra articulatory areas); and horizontal radiographic section (right half) (F), position of the photo at 49.1 mm to the top of the headgear, showing the thick bony wall of *D. xiezhi*. (**G** and **H**) IVPP V26604, a juvenile. (G) The vertical radiographic section of the headgear, position of the photo at 56.5 mm to the rostral-most point of the headgear, in which the pink dotted line shows the discontinuous bone histology, possibly representing the epiphyseal line. (H) The dorsal view of the headgear, emphasizing the surface texture of the radical vascular grooves and pores. (**I** and **J**) IVPP V8602, left P3–M3 (P, upper premolar; M, upper molar), in occlusal (I) and labial (J) views. (**K** and **L**) IVPP V26875, left hemimandible bearing the p2–m3 (p, lower premolar; m, lower molar) tooth row and the alveolus of p1, in occlusal (I) and lingual (J) views. Abbreviations are as follows: a p1, alveolus of p1; bp, basilar platform; c n, nuchal crest; c os, chronic osteomyelitis; eam, external auditory meatus; et, Eustachian tube; f j, jugular foramen; f m, foramen magnum; f n, nuchal fossa; f o, foramen ovale; hg, headgear; iPs, internal parietal sinus; lv, lamina vaginalis; nf P, nutrient foramen of parietal; Op, external occipital protuberance; v ea, extra articulation of cervical vertebrae; vf Oc, ventral fusion of occipital condyles; vg, vascular groove; vp, vascular pore; v vc, ventral chunk of atlas.

enlarged between the other cervical vertebrae) has also been observed in *Ovibos* and its close extinct relatives (*6*) but is less pronounced than that in *D. xiezhi*. Finite element analyses were also conducted in three extant head-butters: *Ovibos*, *Ovis*, and *Pseudois* (Fig. 3, E and F; figs. S4 and S15; movies S1 to S4; and tables S1 to S3). In the time history curves of strain energy of the bony structure, the peak values of extant head-butters are one to five times larger than that of *D. xiezhi*. Furthermore, in the time history curves of strain energy of the endocast, the *D. xiezhi* and *Ovibos* models rapidly diminish to a low magnitude of fluctuation; whereas the *Ovis* and *Pseudois* models exhibited persistent fluctuation at a high magnitude after the first wave (Fig. 3F). The results reveal that the mechanical effects observed in the *D. xiezhi* cranium greatly surpass those of extant head-butters in strain energy absorption and encephalon protection (Fig. 3, E and F, and fig. S15). These biomechanical analyses of specialized head-neck structures suggest that *D. xiezhi* may have exhibited the fiercest head-butting behavior among all ruminants. Furthermore, such a complex head-neck joint has not been reported in other presumed head-butting vertebrates in the fossil record [e.g., *Pachycephalosaurus* or *Moschops* (*7*, *8*)]. Thus, to the best of our knowledge, *D. xiezhi* exhibits the most optimized head-butting adaptation in vertebrate evolution. Furthermore, the presence of pathological structures interpreted as chronic osteomyelitis (*9*) in the headgear of a subadult (Fig. 1H and fig. S6E) may indicate practice of headbutting in young male individuals.

Several key cranial characteristics support the giraffoid affinity of *D. xiezhi*. (i) As in *Giraffa camelopardalis* and sivatheres, the parietal bone participates in major support of the headgear (*10*, *11*) (Fig. 1, and figs. S5 and S6). (ii) Median frontal or parietal headgear is rarely developed in pecorans other than giraffoids (e.g., in *Giraffa*, *Giraffokeryx*, and *Bramatherium*). (iii) In *D. xiezhi*, the discontinuous bony tissue of the headgear in radiographic sections (Fig. 1G) indicates its dermal origin, similar to the giraffid ossicones (*12*). (iv) In the bony labyrinth, the lateral semicircular canal runs parallel to the posterior semicircular canal shortly before the former joins the posterior ampulla. The insertions of the lateral and posterior semicircular canals are almost at the same level. This feature has been shown to be of high phylogenetic relevance in ruminants (*13*). The morphology of *D. xiezhi* is comparable to *Giraffa* and *Okapia* (Fig. 4, A to C) but distinct from that observed in other extant ruminant families. In the extant Antilocapridae, Cervidae, Moschidae, and Bovidae, the insertion of the lateral semicircular canal is higher than that in giraffoids (Fig. 4, E to H).

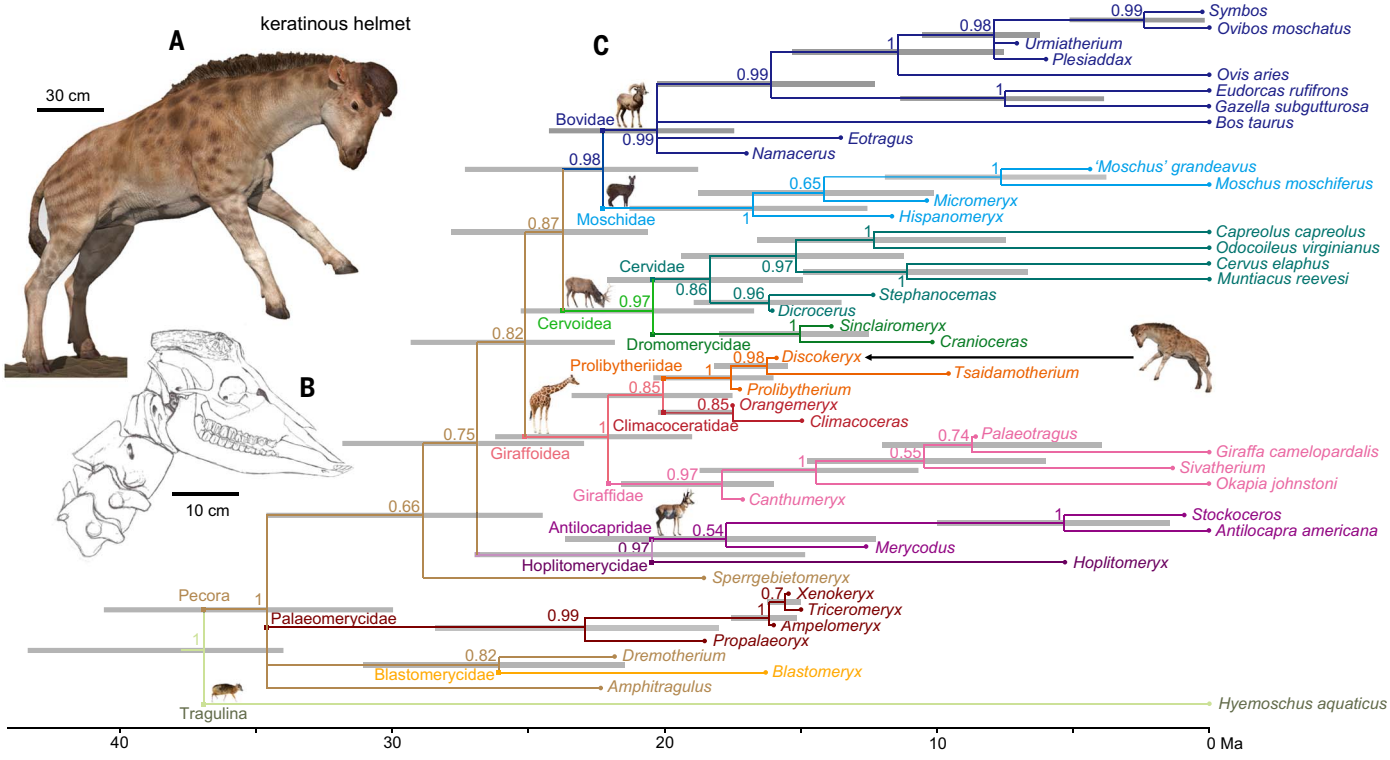

Fig. 2. *D. xiezhi* gen. et sp. nov., reconstruction and phylogeny. (**A**) The 3D digital model of *D. xiezhi*, reconstructed by Y. Wang. (**B**) The reconstruction of the skull and cervical vertebrae of *D. xiezhi* based on IVPP V26602. (**C**) The phylogenetic reconstruction of pecoran ruminants based on morphological and molecular data using the Bayesian total-evidence dating method with the molecular backbone constraint, in which Prolibytheriidae (*Discokeryx*, *Tsaidamotherium*, and *Prolibytherium*) and Climacoceratidae are positioned as the sister groups, which are further clustered with Giraffidae. The node support (the number at each node) is the posterior probability, and the node bars are 95% confidence age intervals. Data sources: data S2 and code file S3.

(v) The histological sections of the headgear demonstrate a lamellar structure with some large-scale osteons, similar to that of some fossil and extant giraffids (*14*) (Fig. 4, I to K, and fig. S11). (vi) As in giraffes (*11*), a large nutrient foramen is present at the centrocaudal part of the parietal bone (Fig. 1E, and fig. S5 and S6). In giraffes, this foramen conducts the cornual vein from the ossicone to the dura mater sinus system (*11*). In *D. xiezhi*, this foramen conducts a canal into the internal parietal sinus (fig. S8), which connects with the superior petrosal sinus of the dura mater sinus system. Furthermore, *D. xiezhi* shares with *Tsaidamotherium* and *Prolibytherium* the ventrally fused occipital condyles and the central development of one single headgear (*15*, *16*) (defining Prolibytheriidae Sánchez *et al.*, 2019) (Fig. 1 and figs. S5 and S6).

The cheek teeth could easily be assigned to *D. xiezhi* by size; *D. xiezhi* is the largest ruminant in the fossil assemblage (Halamagai community) (Fig. 5, inset), and its remains are very abundant in the fossil assemblage (fig. S16A). The teeth are giraffoid-like, with a relatively high crown, resembling those of *Prolibytherium magnieri* (*16*, *17*) (Fig. 1, I to L, and fig. S9). The molarized fourth lower premolar has an anterolingual and a posterolingual cristid, and the two cristids almost enclose the anterior and posterior valleys, respectively. However, the presence of the first lower premolar alveolus in the referred mandible is a plesiomorphic character state among pecorans (Fig. 1K and fig. S9). Finally, lower canines, possibly the most diagnostic element for Giraffoidea (*17*, *18*), have not yet been discovered for *D. xiezhi*.

Bayesian total-evidence dating analyses, with and without the molecular backbone constraint, have resulted in classifying *Discokeryx* and *Tsaidamotherium* as a clade (Discokerycinae) (Fig. 2C and fig. S12). *Tsaidamotherium* was previously thought to be a bovid (*19*). However, it also has a median parietal headgear, which is supported almost solely by the parietal bone and was fused in a stepwise manner with the cranial roof (fig. S5, I and J). These features are absent in Bovidae. In the bony labyrinth (Fig. 4D) of *Tsaidamotherium*, the insertion of the lateral semicircular canal is close to that of the posterior semicircular canal, clearly showing a giraffoid condition. *Prolibytherium* is the sister group of Discokerycinae (Fig. 2C and fig. S12) with a node support of 100%. The above topologies are further supported by the most parsimonious analysis based on morphological data only (fig. S13). In the Bayesian total-evidence dating analyses, Prolibytheriidae + Climacoceratidae is the sister group of Giraffidae, whereas in the most parsimonious analysis, Prolibytheriidae is the sister group of Giraffidae (Fig. 2C and figs. S12 and S13). The clade comprising Prolibytheriidae, Giraffidae, and Climacoceratidae is retained throughout all analyses. In the current study, we considered this clade to be Giraffoidea (Fig. 2C and figs. S12 and S13). The phylogenetic relationships of the crown families are inconsistent in Bayesian total-evidence dating and most parsimonious analyses (Fig. 2C and figs. S12 and S13), and in this study we adopted the phylogeny resulting from the Bayesian total-evidence dating analysis with the molecular backbone constraint (Fig. 2C).

Discussion

In contrast to the low diversity today, with only two extant representatives, fossil giraffoids seems to display more diversity in headgear morphology than any other ruminant group (Table 1 and Fig. 6A). Although it is difficult to establish a satisfactory subdivision for different headgear types in each pecoran group, we attempted to explore headgear variation in different pecoran groups (our results are listed in Table 1). According to our criteria, there are a total of 14 known types of headgear in Giraffomorpha (Giraffoidea + Palaeomerycidae), 13 in Giraffoidea, 9 in Cervoidea, 8 in Antilocapridae + Hoplitomerycidae,

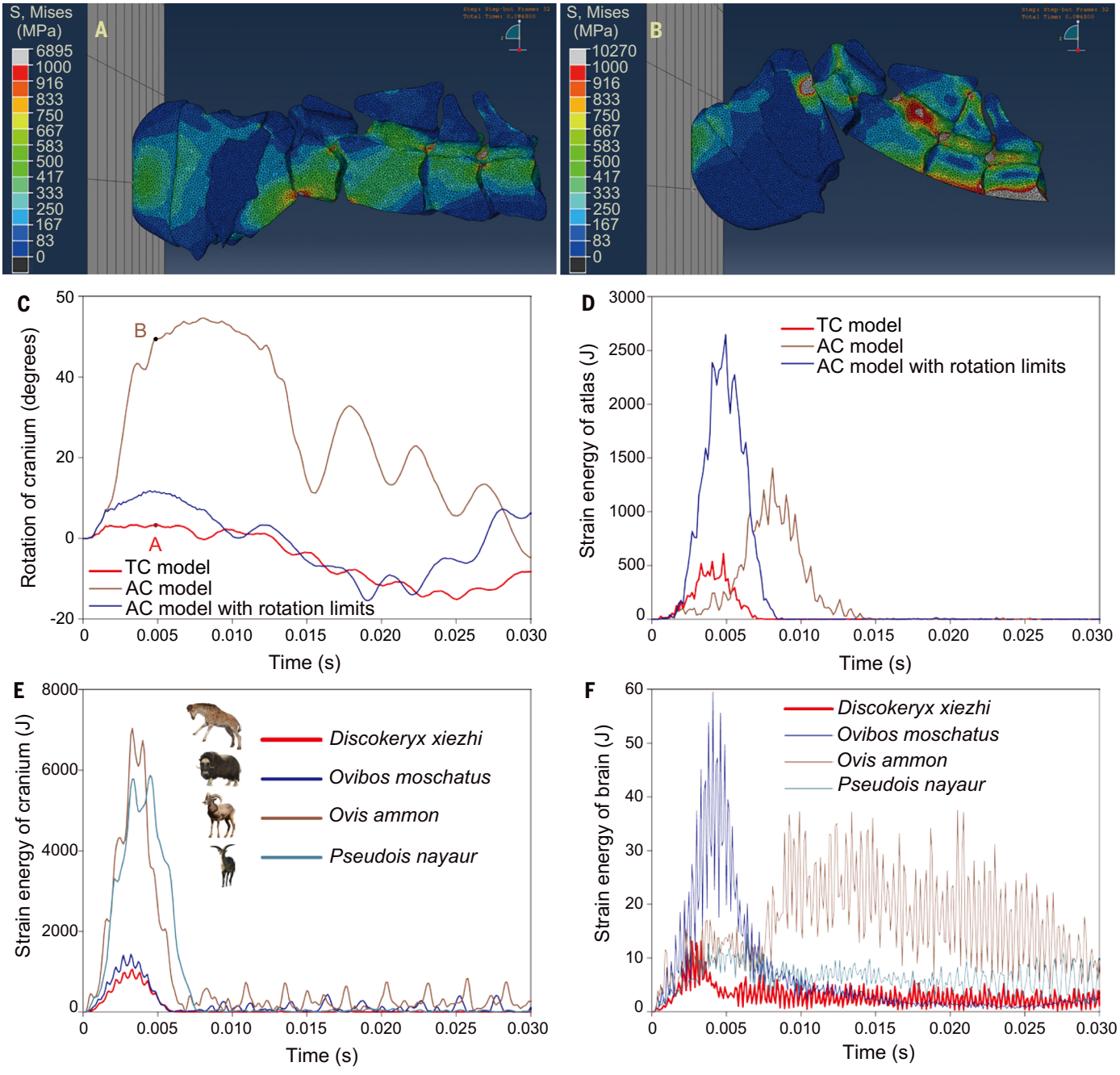

Fig. 3. Finite element (FE) modeling for the head-butting behavior in *D. xiezhi* gen. et sp. nov. and extant bovids. (**A** and **B**) Von Mises stress contour color maps of *D. xiezhi* models in FE head-butting modeling at a typical time point (0.0048 s), in comparison between the thick cervical (TC) model (A) and the attenuated cervical (AC) model (B). In the AC model, the specialized extra articulation between the braincase and atlas and the intervertebral articulations were removed from the TC model. (**C** and **D**) Dynamic responses of *D. xiezhi* models in FE head-butting modeling, in comparison between the TC (red) and AC (brown) models, as well as an AC model with a 5° ventral bending limit of the atlanto-occipital joint (blue). Note that the ventral overbending of the braincase in the AC models was revealed by the rotation curves (C) and the large peak values of THCSE (D). (**E** and **F**) Mechanical responses of *D. xiezhi* compared with extant head-butters. Note that in the *D. xiezhi* model, the strain energy of the cranium peaked at the lowest value (E), and the brain vibration amplitude was the smallest among the four curves (F). Data sources: tables S1 to S3, data S5, code files S1 and S2, Movies 1 to 3, and movies S4 to S7.

and 5 in Bovidae. This might be related to the dermal nature of giraffoid headgear, with strong developmental plasticity and flexibility (*12*). Ossification centers are not constrained in specific areas [such as the tip and out surfaces in bovids (*18*)] and are distributed deeply and widely within the headgear (*14*). Accordingly, the head-neck morphology of giraffoids also varies, especially for the elongation and the thickness of the cervical vertebrae (Fig. 6B and fig. S17A). These findings raise the possibility that the variety of giraffoid headgears as well as the head-neck morphologies were influenced by different combat styles, as postulated for the evolution of headgear in female bovids (*20*). For instance, the evolution of thick cervical vertebrae in *D. xiezhi* was related to head-butting combats, and the evolution of a

Movie 1. FE modeling of *D. xiezhi*, head-neck thick cervical model.

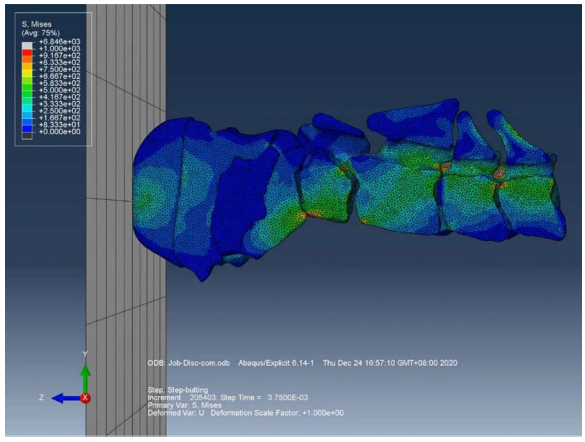

Movie 2. FE modeling of *D. xiezhi*, head-neck attenuated cervical model.

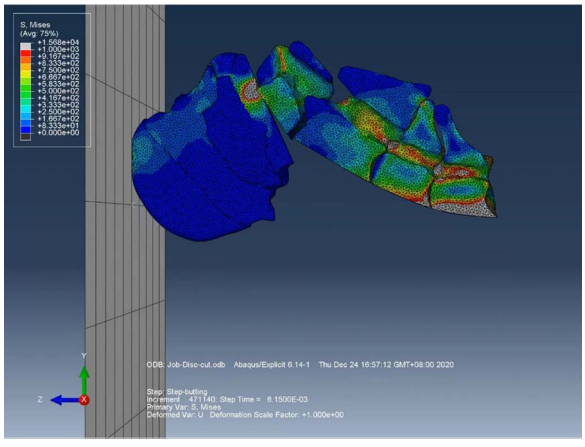

Movie 3. FE modeling of *D. xiezhi*, head-neck attenuated cervical model with a 5° ventral bend limitation.

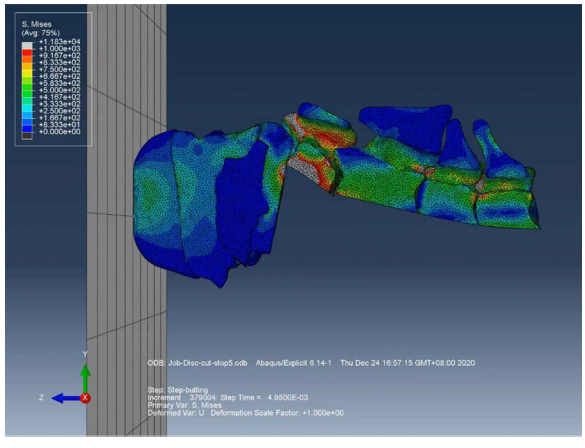

long neck in the recent *Giraffa* might have been influenced by their "necking" combats (*3*, *4*). Here, as in classical case studies, behavior may have strongly affected morphological evolution (*21*), with extreme behavior leading to extreme morphological evolution in giraffoids.

Why did giraffoids diverge in headgear morphology and intensify in combat styles? This divergence may have been influenced by ecological factors. *D. xiezhi* appeared during the mid-Miocene Climate Optimum (*22*) (Fig. 6A), when several new niches opened locally after a long phase of aridity (*23*). As a result, the Halamagai Formation is thought to have had the most abundant ruminant community recognized in the Chinese Neogene (Fig. 5; fig. S16A; and data S3 to S5). Notably, besides *D. xiezhi*, another three giraffoids (one climacoceratid and two giraffids, all unnamed) have been discovered, revealing important and novel aspects of the early radiation of giraffoids (*16*), which has seldom been reported outside of Africa. Isotope analyses of enamel samples from *D. xiezhi* yielded the second highest average $\delta^{13}C$ value (higher than that of contemporary bovids) among all herbivores analyzed in this study and also a large range of $\delta^{18}O$ values (Fig. 6C; fig. S17B; and data S7). The former indicates that *D. xiezhi* was an open-land grazer, and the latter suggests multiple sources of water intake or seasonality of the living habitats. A part of the sample range (the dashed box in Fig. 6C) that does not overlap with that of the other herbivore samples is also distinctly different from all known data from other early-middle Miocene fossil communities of northern China (Fig. 6D). Thus, living habitats of *D. xiezhi* likely included some special areas that were difficult for their contemporary herbivores to make use of. It is also noteworthy that extant head-butters usually live in harsh climates with relatively low productivity in the environment, for example, bighorn sheep in rugged mountains and musk oxen in the tundra (*24*). Therefore, it is possible that *D. xiezhi* might have lived in a marginal niche.

Living giraffes can browse at the highest level in the African savannah woodlands, well outside the reach of other ruminants. Earlier in their evolution, giraffoids were high-level browsers and occupied a niche not available to other smaller contemporary ruminants (*25*). The long necks of giraffes are thought to have emerged in the early Pliocene in savannah areas (*26*), when C_4 ecosystems started being widely established (*27*) (Fig. 6A). "Necking" combat was likely the primary driving force for giraffes who had evolved a long neck, and high-level browsing was likely a compatible benefit of this evolution (*4*). Furthermore, one possible strategy of giraffoids might be avoiding competition from bovids and cervids by taking advantage of some marginal niches in the ecosystem. For example, in the late Miocene Greek locality of Pikermi, microwear data indicate that fossil giraffids covered the ranges of browsers, grazers, and mixfeeders, but these data do not overlap those of bovids (*28*).

Here we have described a newly discovered giraffoid, *D. xiezhi*. This animal had a distinctive disklike headgear combined with a complex head-neck morphology suggesting that it performed fierce head-butting behavior. The evolution of headgear, possibly for use as a weapon in

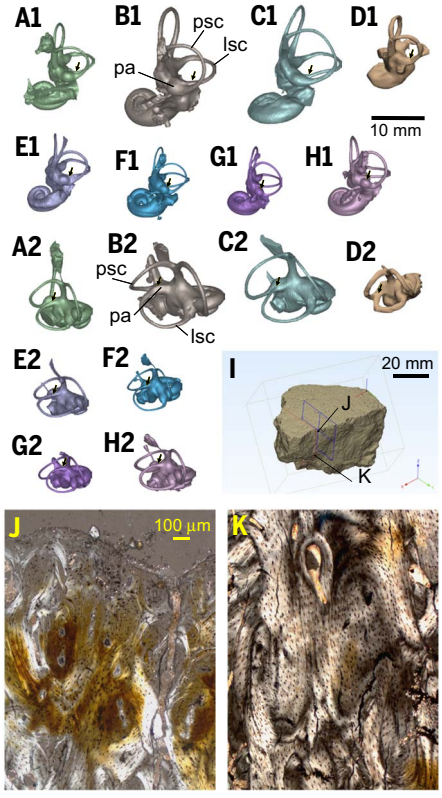

Fig. 4. Bony labyrinths of *D. xiezhi* gen. et sp. nov. in comparison with various pecorans, and headgear histology of *D. xiezhi* gen. et sp. nov. (**A** to **H**) Bony labyrinths of *D. xiezhi* (IVPP V26870) (A), *Giraffa camelopardalis* (IVPP OV 1273) (B), *Okapia johnstoni* (NMB 10811) (C), *Tsaidamotherium hedini* (IVPP RV 35052, type specimen) (D), *Antilocapra americana* (NMB.C.1618) (E), *Muntiacus reevesi* (IVPP OV 593) (F), *Moschus moschiferus* (IVPP OV 1238) (G), and *Gazella subgutturosa* (IVPP OV 574) (H). Panels marked "1" give dorso-occipital views, and those marked "2" give dorso-lateral views, showing the position of insertion and direction of the lateral semicircular canal at the posterior semicircular canal ampulla (black arrows). (**I** to **K**) Histology of IVPP V26783, an incomplete isolated headgear (I), showing the histological slices of the tangent section, at the top margin (**L**) and ~10 mm below the top (**M**), respectively. Abbreviations: lsc, lateral semicircular canal; pa, posterior semicircular canal ampulla; psc, posterior semicircular canal. Data sources: 3D models S9 to S13 (*5*).

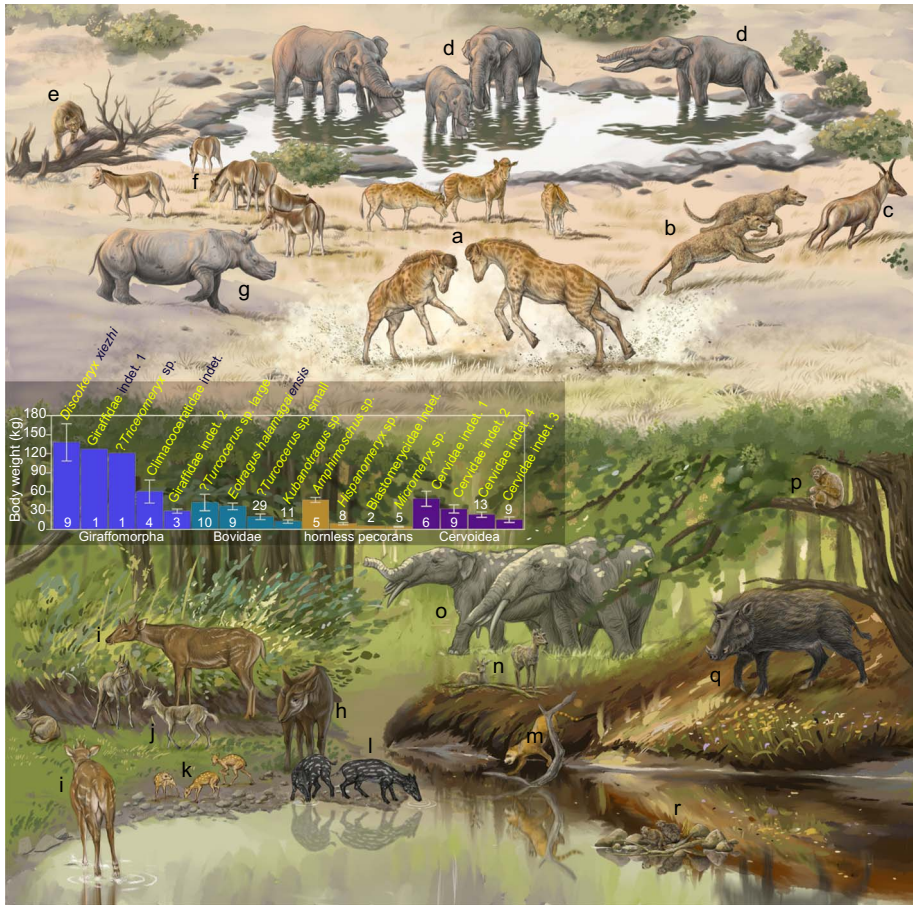

Fig. 5. Scenery reconstruction of the Halamagai community and body mass estimations for ruminants. The numbers in each bar represent the sample size. Lowercase letters correspond to the following: a, *Discokeryx xiezhi* gen. et sp. nov.; b, *Gobicyon zhegalloi*; c, Climacoceratidae indet.; d, *Platybelodon* sp.; e, *Oriensmilus* sp.; f, *Anchitherium gobiensis*; g, *Diaceratherium* sp.; h, Giraffidae indet. 1; i, *?Tricheromeryx* sp.; j, *Eotragus halamagaiensis*; k, *Micromeryx* sp.; l, *Elomeryx* sp.; m, *Alopecocyon* cf. *goeriachensis*; n, *Ligeromeryx* sp.; o, *Gomphotherium* sp.; p, *Pliopithecus bii*; q, *Kubanochoerus* sp.; and r, *Steneofiber depereti*. For details of body mass estimations, see supplementary materials, section 2.8.2. Data sources: data S3 and S4.

intraspecific male competition (*29*), may have played a role as an exaptation to environmental changes (*30*). At the beginning of their radiation, the ecological positioning of giraffoids, which occupied more-marginal niches than cervoids and bovids, likely further influenced their evolutionary strategies. The head-butting *Discokeryx* and "necking" *Giraffa* suggest that sexually related intraspecific reproductive competition led to morphological evolution, by means of which giraffoids actively responded to environmental challenges.

Materials and methods summary

What follows is a brief summary of the materials and methods. For more details, please see section 2 of the supplementary materials.

Materials

Fossil materials are housed at the Institute of Vertebrate Paleontology and Paleoanthropology, Chinese Academy of Sciences (IVPP) (data S1 and S3). The three-dimensional (3D) digital bony labyrinths of the extant ruminants are housed at the IVPP and the Natural History Museum of Basel (NMB). The other data of single measurements were obtained from various institutions, including the IVPP; NMB; American Museum of Natural History (AMNH); Institute of Zoology, Chinese Academy of Sciences (IOZ); Beijing Zoo (BZ); and Beijing Museum of Natural History (BMNH).

Surface 3D digital models were generated using a handheld Artec Spider 3D scanner. The high-resolution computed tomography images were obtained for the petrosal, bony labyrinths, brain endocasts, and internal vascular system of *D. xiezhi* and relevant taxa. The 3D models were reconstructed using VGStudio Max (V3.0) and Mimics Research (V20.0) software.

Finite element analysis

Finite element models (fig. S4, A and B) were designed on the basis of the type specimen (IVPP V26602), including the cranium and four cervical vertebrae. The keratinous helmet was reconstructed with a thickness of ~50 mm, which was the most conservative estimation based on the percentage of horncore length relative to sheath length in extant caprines (*31*) (see supplementary materials, section 2.7.1).

Three different materials with different mechanical properties were used in the models,

Table 1. Occurrence of various headgears in different pecoran groups.

Group	Category	Earliest taxon	Age (Ma)	Refs.
Bovidae	One pair straight horncores	*Eotragus*	18	(*49*)
	One pair curved horncores	*Caprotragoides*	15.5	(*50*)
	One pair twisted horncores	*Hypsodontus*	15.5	(*50*)
	Paired horncores that tend to be fused	*Urmiatherium*	8.2	(*51*)
	Multipaired horncores	*Tetracerus*	0	(*24*)
Cervidae	Branched antlers without a burr or scar	*Acteocemas*, *Ligeromeryx*	~19.6	(*52*, *53*)
	Palmed antlers with a shedding scar	*Stephanocemas*	~19.4	(*52*)
	Branched antlers with a shedding scar	*Dicrocerus*	19.4	(*52*)
	Single-branched antlers with a burr	*Euprox*	~15	(*49*)
	Multibranched antlers with a burr	*Cervavitus*	9.7	(*49*)
	Palmed antlers with a burr	*Proesinomegaceros*	~7.5	(*54*)
Dromomerycidae	Paired unbranched frontal protrusions	*Barbouromeryx*	19.2	(*55*)
	Single unbranched occipital protrusion	*Barbouromeryx*	19.2	(*55*)
	Paired nasal protrusions	*Sinclairomeryx*	17.5	(*55*)
Antilocapridae	Single-branched pseudo-antlers	*Merycodus*	18.8	(*56*)
	Palmed or knobbed pseudo-antlers	*Merriamoceros*	17.5	(*56*)
	Multibranched pseudo-antlers	*Ramoceros*	16.8	(*56*)
	One pair branched pronghorns	*Plioceros*	14.0	(*56*)
	One pair unbranched pronghorns	*Osbornoceros*, *Ilingoceros*	8.8	(*56*)
	Multipaired pronghorns	*Texoceros*, *Hexobelomeryx*	8.8	(*56*)
Hoplitomerycidae	Multipaired "horns" with keratinous integument	*Hoplitomeryx*	~6.6	(*49*)
	Single nasal protrusion	*Hoplitomeryx*	~6.6	(*49*)
Palaeomerycidae	One pair frontal ossicones, dorsally oriented	*Sinomeryx*	18	(*57*, *58*)
	Branched or knobbed occipital protrusion	*Sinomeryx*	18	(*57*, *58*)
Giraffoidae indet.	Two tines, one curved	gen. et sp. indet.	17.9	(*59*)
Climacocerotidae	One pair unbranched frontal protrusions	Climacoceratidae indet.	18	(*16*)
	One pair branched frontal protrusions	*Orangemeryx*	~17.5	(*60*)
Prolibytheriidae	Single palmed ossicone without keratinous integument	*Prolibytherium*	18	(*16*)
	Single disklike ossicone with keratinous integument	*Discokeryx*	16.9	This study
Giraffidae	One pair frontal ossicones, laterally oriented	*Canthumeryx*	18	(*59*)
	Paired frontal ossicones and paired parietal ossicones, separated	*Giraffokeryx*	~14	(*26*, *61*)
	One pair frontal ossicones, dorsally oriented	*Afrikanokeryx*	~12	(*17*, *26*)
	One median branched ossicone and one pair parietal ossicones	*Bramatherium perimensis*	~11	(*61*)
	Two pairs frontal ossicones, roots merged	*Schansitherium*	~10	(*62*)
	Paired frontal ossicones, separated, and paired parietal ossicones, palmed	*Dencennatherium*	~9	(*10*)
	Paired parietal ossicones, straight	*Giraffa*	~5	(*26*)
	Median unbranched ossicone	*Giraffa*	~5	(*26*)

including bone, keratin, and gray matter of the brain (we used the gray matter material to approximate the whole brain). The former two were treated as isotropic linear elastic materials, whereas the latter one was treated as an isotropic hyperelastic-viscoelastic material. The detailed parameters followed Drake *et al.* (*32*) and Wu (*33*) (table S2).

A geometrical treatment was performed on the models—the basilar platform of the cranium, the central chunk of the atlas, and the additional intervertebral articulations formed by the ventral tuberosity of traversal processes and the caudal surface of the preceding vertebra were all removed from the original thick cervical model. We called this adjusted model the attenuated cervical model. The attenuated cervical model represented the ordinary head-neck morphology in the common animals without a head-butting behavior. Finite element analyses were performed on the thick and attenuated cervical models, respectively. A point mass of 0.07 metric tons following the cervical vertebra IV to represent the body mass, and 0.07 tons as half of 140 kg, following the body mass regression of type specimen (IVPP V26602) of *D. xiezhi*, 154.5 kg minus the mass of the cranium and cervical vertebrae (fig. S16B and data S4 and S5). A constant velocity field, 22,222 mm/s, was predefined. This velocity (the relative velocity between the two head-butting animals) is twice that exhibited by extant *Ovibos moschatus* during a typical head-butting performance (~40 km hour^{-1}) (*24*). The results were reported in the time series of the strain energy in various parts of the model and the von Mises stress contour color maps of the models at particular time points and animations of head-butting processes (code file S1).

Finite element models of *Ovis ammon*, *Pseudois nayaur*, and *Ovibos moschatus* were also designed. Only the skull and body mass were assembled in the models (fig. S4, C to F). All of the models were scaled into similar dimensions, with the half cranial width equal to 60 mm to facilitate comparison. Each body mass was set as 0.07 tons, with the same initial velocity of 22,222 mm/s. The other settings and result reports were the same as the head-neck models in *D. xiezhi* (code file S2).

Histological sample preparation

An isolated headgear of *D. xiezhi* (IVPP V26873), a giraffid ossicone of a *Honanotherium schlosseri*

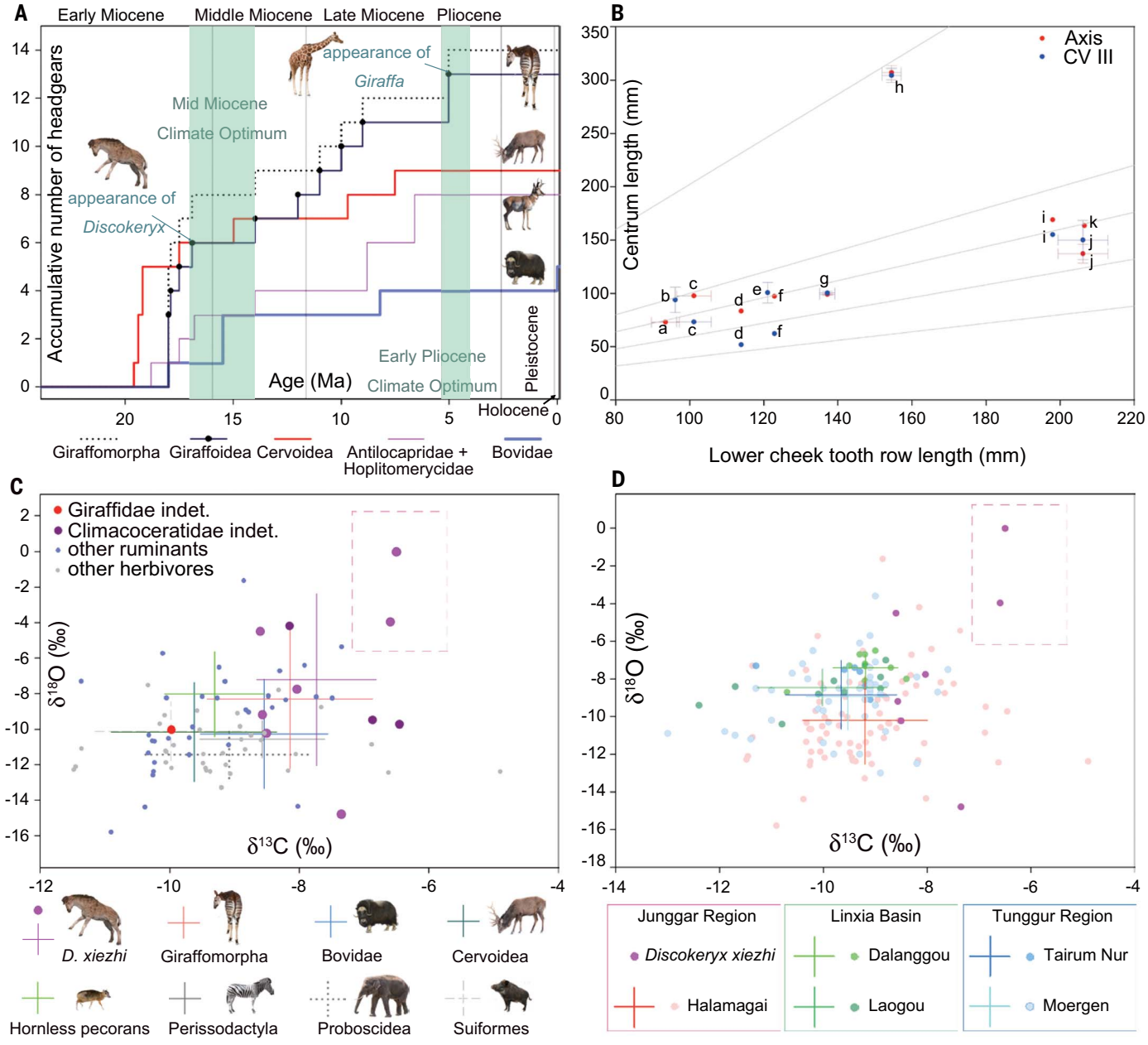

Fig. 6. Head-neck morphology and ecology of ruminants. (**A**) Headgear diversity (accumulative numbers, shown as step lines) of ruminant groups during the late Neogene, in which the giraffoids exhibited more diversity in headgear morphology than the other pecoran groups; notably, both *Discokeryx* and *Giraffa* appeared during important paleoenvironment events. Giraffomorpha = Giraffoidae + Palaeomerycidae, sensu Sánchez *et al*., 2015. (**B**) Morphological variations of the giraffoid axis and the third cervical vertebra, in which the sample points represent the average centrum length (the vertical coordinate) versus average lower cheek tooth row length in each taxon (the horizontal coordinate) (error bars represent standard deviations). Lowercase letters correspond to the following: a, *Climacoceras gentryi*; b, *Giraffokeryx punjabiensis*; c, *Orangemeryx hendeyi*; d, *Decennatherium rex*; e, *Canthumeryx sirtensis*; f, *D. xiezhi* gen. et sp. nov.; g, *Okapia johnstoni*; h, *Giraffa camelopardalis*; i, *Samotherium sinense*; j, *Samotherium major*; and k, *Bramatherium megacephalum*). (**C**) Stable isotope ratios of the tooth enamel in the Halamagai herbivore community, the crosses representing the standard deviations, and (**D**) those of the early-middle Miocene communities from northern China [data from Wang and Deng and Zhang *et al*. (*47*, *48*)]. The dashed box indicates the area occupied by *D. xiezhi*, showing no overlap with other herbivores, which suggests that *D. xiezhi* may have occupied different niches than its contemporary herbivores. Data sources: Table 1 and data S6 and S7.

(unnumbered IVPP specimen), and a bovid horncore of ?*Turcocerus* sp. (small form) were sectioned tangentially and horizontally using standard techniques. The specimens were cut into small pieces and embedded in resin and then further sectioned using a professional cutting system, resulting in thin slices (~8 to 10 μm). Histological slices were observed and imaged using a polarized light microscope.

Cladistic analysis

Cladistic analyses were performed to test the phylogenetic hypothesis among various pecoran groups. The data matrix contains 45 taxa, in which *Hyemoschus aquaticus* was selected as the outgroup. The characters are combined with morphological and DNA data. The 110 morphological characters (data S2) were based on several references (*13*, *18*, *25*, *34*, *35*) and self-compiled; and the DNA data were from Hassanin *et al*. (*36*). Two methods, Bayesian

total-evidence dating and most parsimonious analyses, were performed. The most parsimonious reconstruction was performed by the program TNT1.1 (*37*), in which only morphological dataset (data S2) was used. The molecular and morphological data were used in Bayesian total-evidence dating analysis performed by MrBayes 3.2.7 (*38*), in which a backbone constraint for the extant taxa based merely on the molecular data (*36*) was or was not enforced (code files S3 to S5).

Ecology investigations

Various headgear types in terms of development and morphology were examined, including the following groups: Bovidae, Cervidae, Antilocapridae + Hoplitomerycidae, and Giraffoidea/Giraffomorpha (Fig. 6A). In our scheme, the following aspects were considered: (i) support element (nasal, frontal, parietal, or occipital); (ii) position on the cranial roof (supraorbital, postorbital, or central); (iii) number of the frontal appendages (single, double, triple, quadruple, or sextuple); (iv) covering in the mature state (skin, keratin, or naked); (v) morphology (spike-like, branched, palmed, or combined multiforms); (vi) nondeciduous or deciduous; (vii) presence or absence of burr in antler; and (viii) fusion of horncores. The appearance of each headgear type in geological time was drawn in step lines showing the cumulative number in each pecoran group (Table 1).

We investigated the relative length and thickness of axes and cervical vertebrae III among various giraffoid taxa. The arithmetic means of centrum length and cheek teeth row length were used for generating a bivariate diagram of cheek teeth row length versus centrum length. The ratio of minimal width to centrum length of axes and cervical vertebrae III in giraffoids were also calculated and plotted. Data were from previous publications (*10*, *17*, *39*–*46*).

In total, 81 enamel samples were collected from teeth of the Halamagai herbivore community for $\delta^{13}C$ and $\delta^{18}O$ measurements (data S7), including ruminants, proboscideans, suids, rhinocerotids, and equids. Results are reported in standard delta (δ) notation as $\delta^{13}C$ and $\delta^{18}O$ values in reference to the international carbonate standard Vienna Pee Dee belemnite. Stable isotope data from other herbivore communities from the early-middle Miocene of northern China were obtained from literature (*47*, *48*). All these data (including the previously published data) were conducted at the National High Magnetic Field Laboratory, Florida State University, USA.

REFERENCES AND NOTES

1. C. Darwin, *The Descent of Man, and Selection in Relation to Sex* (David McKay, new ed., 1874).
2. J.-B. Lamarck, *Philosophie Zoologique, vol. 1* (Duminil-Lesueur, 1809).
3. R. E. Simmons, R. Altwegg, Necks-for-sex or competing browsers? A critique of ideas on the evolution of giraffe. *J. Zool.* **282**, 6–12 (2010). doi: 10.1111/j.1469-7998.2010.00711.x
4. R. E. Simmons, L. Scheepers, Winning by a neck: Sexual selection in the evolution of giraffe. *Am. Nat.* **148**, 771–786 (1996). doi: 10.1086/285955
5. S.-Q. Wang *et al*., Supplementary 3D Models of *Discokeryx xiezhi*. Dryad (2022); https://doi.org/10.5061/dryad.dncjsxm0j.
6. B. Bohlin, Cavicornier der *Hipparion*-Fauna Nord-Chinas. *Palaeontol. Sin. C* **9**, 1–166 (1935).
7. J. Benoit, P. R. Manger, L. Norton, V. Fernandez, B. S. Rubidge, Synchrotron scanning reveals the palaeoneurology of the head-butting *Moschops capensis* (Therapsida, Dinocephalia). *PeerJ* **5**, e3496 (2017). doi: 10.7717/peerj.3496; pmid: 28828230
8. E. Snively, A. Cox, Structural mechanics of pachycephalosaur crania permitted head-butting behavior. *Palaeontol. Electronica* **11**, 3A (2008).
9. J. E. Peterson, C. Dischler, N. R. Longrich, Distributions of cranial pathologies provide evidence for head-butting in dome-headed dinosaurs (Pachycephalosauridae). *PLOS ONE* **8**, e68620 (2013). doi: 10.1371/journal.pone.0068620; pmid: 23874691
10. M. Ríos, I. M. Sánchez, J. Morales, A new giraffid (Mammalia, Ruminantia, Pecora) from the late Miocene of Spain, and the evolution of the sivathere-samothere lineage. *PLOS ONE* **12**, e0185378 (2017). doi: 10.1371/journal.pone.0185378; pmid: 29091914
11. C. A. Spinage, Horns and other bony structures of the skull of the giraffe, and their functional significance. *Afr. J. Ecol.* **6**, 53–61 (1968). doi: 10.1111/j.1365-2028.1968.tb00900.x
12. E. B. Davis, K. A. Brakora, A. H. Lee, Evolution of ruminant headgear: A review. *Proc. Biol. Sci.* **278**, 2857–2865 (2011). doi: 10.1098/rspb.2011.0938; pmid: 21733893
13. B. Mennecart, G. Métais, L. Costeur, L. Ginsburg, G. E. Rössner, Reassessment of the enigmatic ruminant Miocene genus *Amphimoschus* Bourgeois, 1873 (Mammalia, Artiodactyla, Pecora). *PLOS ONE* **16**, e0244661 (2021). doi: 10.1371/journal.pone.0244661; pmid: 33513144
14. T. Ganey, J. Ogden, J. Olsen, Development of the giraffe horn and its blood supply. *Anat. Rec.* **227**, 497–507 (1990). doi: 10.1002/ar.1092270413; pmid: 2393101
15. M. Danowitz, R. Domalski, N. Solounias, A new species of *Prolibytherium* (Ruminantia, Mammalia) from Pakistan, and the functional implications of an atypical atlanto-occipital morphology. *J. Mamm. Evol.* **23**, 201–207 (2016). doi: 10.1007/s10914-015-9307-8
16. W. R. Hamilton, The lower Miocene ruminants of Gebel Zelten, Libya. *Bull. Br. Mus.* **21**, 73–150 (1973).
17. W. R. Hamilton, Fossil giraffes from the Miocene of Africa and a revision of the phylogeny of the Giraffoidea. *Philos. Trans. R. Soc. London Ser. B* **283**, 165–229 (1978). doi: 10.1098/rstb.1978.0019
18. C. M. Janis, K. M. Scott, The interrelationships of higher ruminant families with special emphasis on the members of the Cervoidea. *Am. Mus. Novit.* **2893**, 1–85 (1987).
19. B. Bohlin, *Tsaidamotherium hedini*, n. g., n. sp. Ein Einhörniger Ovibovine, aus den Tertiären Ablagerungen aus der Gegend des Tossun nor, Tsaidam. *Geogr. Ann.* **17**, 66–74 (1935). doi: 10.2307/519848
20. T. Stankowich, T. Caro, Evolution of weaponry in female bovids. *Proc. Biol. Sci.* **276**, 4329–4334 (2009). doi: 10.1098/rspb.2009.1256; pmid: 19759035
21. A. M. Lister, Behavioural leads in evolution: Evidence from the fossil record. *Biol. J. Linn. Soc. Lond.* **112**, 315–331 (2014). doi: 10.1111/bij.12173
22. J. Zachos, M. Pagani, L. Sloan, E. Thomas, K. Billups, Trends, rhythms, and aberrations in global climate 65 Ma to present. *Science* **292**, 686–693 (2001). doi: 10.1126/science.1059412; pmid: 11326091
23. J. Sun *et al*., Late Oligocene–Miocene mid-latitude aridification and wind patterns in the Asian interior. *Geology* **38**, 515–518 (2010). doi: 10.1130/G30776.1
24. J. R. Castelló, *Bovids of the World: Antelopes, Gazelles, Cattle, Goats, Sheep, and Relatives* (Princeton Univ. Press, 2016).
25. N. Solounias, "Family Giraffidae" in *The Evolution of Artiodactyls*, D. R. Prothero, S. E. Foss, Eds. (Johns Hopkins Univ. Press, 2007), chap. 21.
26. J. M. Harris, N. Solounias, D. Geraads, "Giraffoidea" in *Cenozoic Mammals of Africa*, L. Werdelin, W. J. Sanders, Eds. (UC Press, 2010), chap. 39.
27. T. E. Cerling *et al*., Global vegetation change through the Miocene/Pliocene boundary. *Nature* **389**, 153–158 (1997). doi: 10.1038/38229
28. N. Solounias, F. Rivals, G. M. Semprebon, Dietary interpretation and paleoecology of herbivores from Pikermi and Samos (late Miocene of Greece). *Paleobiology* **36**, 113–136 (2010). doi: 10.1666/0094-8373-36.1.113
29. D. J. Emlen, The evolution of animal weapons. *Annu. Rev. Ecol. Evol. Syst.* **39**, 387–413 (2008). doi: 10.1146/annurev.ecolsys.39.110707.173502
30. C. M. Janis, Evolution of horns in ungulates: Ecology and paleoecology. *Biol. Rev. Camb. Philos. Soc.* **57**, 261–318 (1982). doi: 10.1111/j.1469-185X.1982.tb00370.x
31. A. B. Bubenik, "Epigenetical, morphological, physiological, and behavioral aspects of evolution of horns, pronghorns, and antlers" in *Horns, Pronghorns, and Antlers: Evolution, Morphology, Physiology, and Social Significance*, G. A. Bubenik, A. B. Bubenik, Eds. (Springer-Verlag, 1990), chap. 1.
32. A. Drake *et al*., Horn and horn core trabecular bone of bighorn sheep rams absorbs impact energy and reduces brain cavity accelerations during high impact ramming of the skull. *Acta Biomater.* **44**, 41–50 (2016). doi: 10.1016/j.actbio.2016.08.019; pmid: 27544811
33. F. Wu, thesis, Dalian University of Technology (2016).
34. I. M. Sánchez, M. S. Domingo, J. Morales, The genus *Hispanomeryx* (Mammalia, Ruminantia, Moschidae) and its bearing on musk deer phylogeny and systematics. *Palaeontology* **53**, 1023–1047 (2010). doi: 10.1111/j.1475-4983.2010.00992.x
35. I. M. Sánchez, J. L. Cantalapiedra, M. Ríos, V. Quiralte, J. Morales, Systematics and evolution of the Miocene three-horned palaeomerycid ruminants (Mammalia, Cetartiodactyla). *PLOS ONE* **10**, e0143034 (2015). doi: 10.1371/journal.pone.0143034; pmid: 26630174
36. A. Hassanin *et al*., Pattern and timing of diversification of Cetartiodactyla (Mammalia, Laurasiatheria), as revealed by a comprehensive analysis of mitochondrial genomes. *C. R. Biol.* **335**, 32–50 (2012). doi: 10.1016/j.crvi.2011.11.002; pmid: 22226162
37. P. A. Goloboff, J. S. Farris, K. C. Nixon, TNT, a free program for phylogenetic analysis. *Cladistics* **24**, 774–786 (2008). doi: 10.1111/j.1096-0031.2008.00217.x
38. F. Ronquist *et al*., MrBayes 3.2: Efficient Bayesian phylogenetic inference and model choice across a large model space. *Syst. Biol.* **61**, 539–542 (2012). doi: 10.1093/sysbio/sys029; pmid: 22357727
39. J. Morales, D. Soria, M. Nieto, P. Pelaez-Campomanes, M. Pickford, New data regarding *Orangemeryx hendeyi* Morales et al., 2000, from the type locality, Arrisdrift, Namibia. *Memoir Geol. Surv. Namibia* **19**, 305–344 (2003).
40. E. R. Lankester, *Monograph of the Okapi* (British Museum, 1910).
41. D. S. Kostopoulos, The Late Miocene mammal faunas of the Mytilinii Basin, Samos Island, Greece: New collection. *Beitr. Paläont.* **31**, 299–343 (2009).
42. M. Danowitz, A. Vasilyev, V. Kortlandt, N. Solounias, Fossil evidence and stages of elongation of the *Giraffa camelopardalis* neck. *R. Soc. Open Sci.* **2**, 150393 (2015). doi: 10.1098/rsos.150393; pmid: 26587249
43. M. Danowitz, N. Solounias, The cervical osteology of *Okapia johnstoni* and *Giraffa camelopardalis*. *PLOS ONE* **10**, e0136552 (2015). doi: 10.1371/journal.pone.0136552; pmid: 26302156
44. E. H. Colbert, Siwalik mammals in the American Museum of Natural History. *Trans. Am. Philos. Soc.* **26**, 1–401 (1935). doi: 10.2307/1005467
45. E. H. Colbert, A skull and mandible of *Giraffokeryx punjabiensis* Pilgrim. *Am. Mus. Novit.* **632**, 1–14 (1933).
46. B. Bohlin, Die Familie Giraffidae mit Besonderer Berücksichtigung der fossilen Formen aus China. *Palaeontol. Sin. C* **4**, 1–178 (1926).
47. Y. Wang, T. Deng, A 25 m.y. isotopic record of paleodiet and environmental change from fossil mammals and paleosols from the NE margin of the Tibetan Plateau. *Earth Planet. Sci. Lett.* **236**, 322–338 (2005). doi: 10.1016/j.epsl.2005.05.006
48. C. Zhang *et al*., C_4 expansion in the central Inner Mongolia during the latest Miocene and early Pliocene. *Earth Planet. Sci. Lett.* **287**, 311–319 (2009). doi: 10.1016/j.epsl.2009.08.025
49. A. W. Gentry, G. E. Rössner, E. P. J. Heizmann, "Suborder Ruminantia" in *The Miocene Land Mammals of Europe*, G. E. Rössner, K. Heissig, Eds. (Verlag Dr. Friedrich Pfeil, 1999), chap. 23.
50. M. Köhler, Boviden des türkischen Miozäns (Känozoikum und Braunkohlen der Türkei). *Paleontol. Evol.* **21**, 133–246 (1987).
51. M. Mirzaie Ataabadi, R. Bernor, D. S. Kostopoulos, "Recent advances in paleobiological research of the Late Miocene Maragheh Fauna, northwest Iran" in *Neogene Terrestrial Mammalian*

Biostratigraphy and Chronology of Asia, X. Wang, L. J. Flynn, M. Fortelius, Eds. (Columbia Univ. Press, 2013), chap. 25.
52. X. Wang *et al*., Biostratigraphy, magnetostratigraphy, and geochronology of lower Miocene Aoerban strata in Central Inner Mongolia. *Palaeogeogr. Palaeoclimatol. Palaeoecol.* **518**, 187–205 (2019). doi: 10.1016/j.palaeo.2018.12.006
53. B. Azanza, Los Cervidae (Artiodactyla, Mammalia) del Mioceno de las cuencas del Duero, Tajo, Calatayud-Teruel y Levante. *Mem. Mus. Paleontol. Univ. Zarag.* **8**, 1–376 (2000).
54. I. A. Vislobokova, A new species of Megacerini (Cervidae, Artiodactyla) from the Late Miocene of Taralyk-Cher, Tuva (Russia), and remarks on the relationships of the group. *Geobios* **42**, 397–410 (2009). doi: 10.1016/j.geobios.2008.12.004
55. C. M. Janis, E. Manning, "Dromomerycidae" in *Evolution of Tertiary Mammals of Norther American. Volume 1: Terrestrial Canivores, Ungulates, and Ungulatelike Mammals*, C. M. Janis, K. M. Scott, L. L. Jacobs, Eds. (Cambridge Univ. Press, 1998), chap. 32.
56. C. M. Janis, E. Manning, "Antilocapridae" in *Evolution of Tertiary Mammals of Norther American. Volume 1: Terrestrial Canivores, Ungulates, and Ungulatelike Mammals*, C. M. Janis, K. M. Scott, L. L. Jacobs, Eds. (Cambridge Univ. Press, 1998), chap. 33.
57. H. He *et al*., New $^{40}Ar/^{39}Ar$ dating results from the Shanwang Basin, eastern China: Constraints on the age of the Shanwang Formation and associated biota. *Phys. Earth Planet. Inter.* **187**, 66–75 (2011). doi: 10.1016/j.pepi.2011.05.002
58. Z. X. Qiu, D. F. Yan, H. Jia, B. Sun, Preliminary observations on the newly found skeletons of *Palaeomeryx* from Shanwang, Shandong. *Vert. PalAsiat.* **23**, 173–200 (1985).
59. A. Grossman, N. Solounias, New fossils of Giraffoidea (Mammalia: Artiodactyla) from the Lothiodok Formation (Kalodirr Member, Early Miocene, West Turkana, Kenya) contribute to our understanding of early giraffoid diversity. *Zitteliana B* **32**, 63–70 (2014). doi: 10.5282/ubm/epub.22387
60. J. Morales, D. Soria, M. Pickford, New stem giraffoid ruminants from the Early and Middle Miocene of Namibia. *Geodiversitas* **21**, 229–253 (1999).
61. J. C. Barry *et al*., Faunal and environmental change in the Late Miocene Siwaliks of northern Pakistan. *Paleobiology* **28** (suppl.), 1–71 (2002). doi: 10.1666/0094-8373(2002)28[1:FAECIT]2.0.CO;2
62. S. Hou, M. Cydylo, M. Danowitz, N. Solounias, Comparisons of *Schansitherium tafeli* with *Samotherium boissieri* (Giraffidae, Mammalia) from the Late Miocene of Gansu Province, China. *PLOS ONE* **14**, e0211797 (2019). doi: 10.1371/journal.pone.0211797; pmid: 30753231

ACKNOWLEDGMENTS

We thank IVPP members Y. Wang for 3D reconstruction; S. Hou, Q. Shi, B. Sun, and Q. Jiangzuo for discussion and suggestions; J. Ma for isotopes explanation; X. Zhou and J. Wang for discussion of paleoenvironment of the Halamagai Formation; S. Li and D. Su for specimens preparation and casts reproduction; Q. Zhao and S. Zhang for histology preparation and discussion; X. Guo for scenery restorative drawing; Y. Hou and S. Wang for 3D reconstruction; W. Gao for taking photos; D. Li for preparing extant specimens; and X. Zhu (IOZ, CAS), Y. Zhang and X. Xia (BMNH), and H. Li (BZ) for assessment of extant specimens. We thank B. Knight from Liwen Bianji (Edanz) (www.liwenbianji.cn/) for editing the English text of a draft of this manuscript. The fieldwork was supported by the Second Comprehensive Scientific Expedition on the Tibetan Plateau 2019QZKK0705. Stable isotope sample preparation and analyses were performed at the National High Magnetic Field Laboratory, which is supported by US National Science Foundation Cooperative Agreement No. DMR-1644779 and the state of Florida. **Funding:** Funding was provided by the Strategic Priority Research Program of the Chinese Academy of Sciences (XDB26000000, XDA20070203, and XDA20070301); the National Natural Science Foundation of China (41872001, 41625005, 52178141, and 41877427); Swiss National Science Foundation projects P300P2_161065, P3P3P2_161066, 200021_178853, 200021_159854/1, and 200021-178853; National Institute of Health Research UK; US National Science Foundation Cooperative Agreement DMR-1157490 and the state of Florida; and Youth Innovation Promotion Association of Chinese Academy of Sciences 2018099. **Author contributions:** Conceptualization: S.-Q.W., J.Y., J.M., and T.D. Three-dimensional reconstruction: S.-Q.W., C.L., L.C., and B.M. Cladistic analyses: S.-Q.W., C.Z., L.C., B.M., and M.A. Finite element analysis: S.-Q.W. and J.Z. Isotope investigation: C.L., Y.Wa., and Y.Wu. Data collection and stratigraphy: J.Y., J.M., W.-Y.W., and S.-Q.W. Writing – original draft: S.-Q.W., J.Y., and J.M. Writing – review & editing: all authors. **Competing interests:** Authors declare that they have no competing interests. **Data and materials availability:** Three-dimensional models S1 to S21 are available in Dryad (*5*). All other data are available in the main text or the supplementary materials.

SUPPLEMENTARY MATERIALS

Submitted 10 August 2021; accepted 28 April 2022
10.1126/science.abl8316

Sexual selection promotes giraffoid head-neck evolution and ecological adaptation

Shi-Qi WangJie YeJin MengChunxiao LiLoïc CosteurBastien MennecartChi ZhangJi ZhangManuela AiglstorferYang WangYan WuWen-Yu WuTao Deng

Science, 376 (6597), eabl8316. • DOI: 10.1126/science.abl8316

Fierce fighters

Since Darwin's time, the giraffe has been held up as a classic example of adaptive evolution. The fact that they browse high in the canopy, due to their long necks, has been considered a direct result of selection for this form of foraging. Wang *et al*. describe a new Miocene giraffoid species with helmet-like headgear and complex head and neck joints indicative of intense head-butting combat. They argue that selection for such combat also played a role in shaping the group's long necks. —SNV